Foundations of factor analysis of medical image sequences: a unified approach and some practical implications

H Benali, I Buvat, F Frouin, J P Bazin and R Di Paola

Factor Analysis of Medical Image Sequences (FAMIS) is presently conducted either in the function space or in the image space. A unified approach jointly using these two spaces is presented. First, the solution of a statistical model for scintigraphic image sequences leads to the use of correspondence analysis which is the optimal orthogonal decomposition of this data. Then, two symmetrical hypotheses concerning either the underlying fundamental functions or the underlying fundamental spatial distributions are derived. These hypotheses are merged in an original method to solve FAMIS physical model. Using this unified approach, *a priori* knowledge about functions and images can be jointly taken into account to improve the estimation of the underlying structures. Some practical applications of the method are illustrated on simulated data.

Keywords: factor analysis of medical image sequences, fixed effect model, target apex seeking

Factor Analysis of Medical Image Sequences (FAMIS) aims at resolving a medical image sequence into its underlying fundamental structures, namely fundamental functions and fundamental spatial distributions having a physical or physiological meaning. It is particularly used in dynamic studies to estimate the variation of concentration of a tracer or a contrast medium within different physiological structures[1-6]. More recently, FAMIS has had a renewal of interest to separate scatter and photopeak photons from a sequence of energy-indexed scintigraphic images[7-9].

FAMIS is based on an additive linear model. This model assumes that the processed medical image sequence consists of a restricted number of overlapping or not overlapping fundamental spatial distributions, each one corresponding to a specific signal variation, called a *fundamental function* (a kinetic for dynamic studies or a spectrum of photons for sequences of energy-indexed scintigraphic images). Such a model is solved by means of an orthogonal analysis followed by an oblique analysis, and numerous methods have been proposed to conduct these two steps:

- The orthogonal analysis aims at determining a study space in which the data is properly represented, whereas the noise is not restored. It always consists of a normalization of the data followed by a principal component analysis. However, various normalizations have been used without theoretical justification[1,3,7,10-13].
- The oblique analysis estimates the fundamental structures (functions and spatial distributions). This analysis is always performed in the function space, except by Samal *et al.*[11,14,15], who considers the image space. The link between the underlying hypotheses of these two approaches has not been

U66 INSERM, Institute Gustave-Roussy, 94805 Villejuif Cedex, France

Paper received: 5 November 1993; revised paper received 24 February 1994

0262-8856/94/06/0375–11

stated yet. Different methods have also been described for using *a priori* knowledge other than the non-negativity of the fundamental structures to overcome the problem of non-uniqueness of the solution of oblique analysis. This knowledge is related either to the fundamental functions or to the fundamental spatial distributions, but there is presently no method using these two kinds of information.

In this paper, a statistical model for medical image sequences is proposed. The solution to this model leads to the determination of the optimal metric (i.e. normalization) for the orthogonal analysis. When processing scintigraphic data, we show that the comparison of the result of the optimal orthogonal decomposition with the physical model of FAMIS suggests two symmetrical hypotheses, which can be merged in a single method to solve FAMIS model. This symmetrical approach unifies some different views proposed up to now: solution in the function space and in the image space is jointly carried out, and *a priori* knowledge related to both fundamental functions and fundamental spatial distributions can be taken into account within the same analysis. The practical applications of the method are illustrated on simulated data. We emphasize the interest of the joint use of *a priori* knowledge about functions and images to achieve a better qualitative and quantitative estimation of the underlying fundamental structures.

STATISTICAL MODEL FOR OPTIMAL ORTHOGONAL ANALYSIS IN FAMIS

Fixed effect model

A sequence of P images, each having N pixels, can be considered as a set of N vectors x_i $(i = 1 \ldots N)$ of P components x_{ij} $(j = 1 \ldots P)$. x_i is called a *trixel*, and represents the variation of the signal within the pixel i in the image sequence indexed by the variable j. Let y_i be a P dimensional vector obtained from a transformation g of x_i, $y_i = g(x_i)$.

The fixed effect model is defined as follows[16]:

- vectors y_i are N independent random vectors defined on a probability space and can be written: $y_i = \tilde{y}_i + \sigma e_i$, where $\tilde{y}_i$ is the fixed effect of y_i and σe_i is the random error;
- the expectation of y_i is $\tilde{y}_i$, $E(y_i) = \tilde{y}_i$, that is $E(e_i) = 0$;
- the variance of y_i can be written

$$\mathrm{Var}(y_i) = \frac{\sigma^2}{\omega_i}\Gamma \tag{1}$$

where Γ is a (P, P) symmetric positive definite matrix assumed to be known as well as the positive numbers ω_i. ω_i is a weight associated to y_i.

- there exists a Q dimensional subspace $\mathbb{S}$ of $\mathbb{R}^P$ $(Q < P)$ such that all $\tilde{y}_i$ belong to $\mathbb{S}$.

The unknown parameters are the subspace $\mathbb{S}$, the N vectors $\tilde{y}_i$ belonging to $\mathbb{S}$ and the parameter σ.

Solution to the fixed effect model

The least square estimate of $\mathbb{S}$ is obtained by minimizing

$$\sum_{i=1}^{N} \omega_i \|y_i - \tilde{y}_i\|^2_{\mathbf{M}} \tag{2}$$

where $\mathbf{M}$ is a (P, P) symmetric positive definite matrix, defining a metric of $\mathbb{R}^P$. It has been shown that the minimum of equation (2) is reached for $\mathbb{S}$ such that[16]:

- $\mathbb{S}$ contains $\bar{y}$, defined by:

$$\bar{y} = \frac{1}{\sum_{i=1}^{N} \omega_i} \sum_{i=1}^{N} \omega_i y_i$$

- $\mathbb{S}$ is spanned by the Q eigenvectors φ_q associated with the Q largest eigenvalues λ_q of the matrix $(\mathbf{Y} - 1_N\bar{\mathbf{Y}})'\mathbf{W}(\mathbf{Y} - 1_N\bar{\mathbf{Y}})\mathbf{M}$, where $\mathbf{Y}$ is the (N, P) matrix of the trixels y_i, $\bar{\mathbf{Y}}$ is the $(1, P)$ matrix of $\bar{y}$, 1_N is a $(N, 1)$ matrix of ones, $\mathbf{W}$ is the (N, N) diagonal matrix of the weights ω_i and t denotes the transpose.

Consequently, $\mathbb{S}$ depends on the metric $\mathbf{M}$. For σ small enough, the perturbation theory can be used to show that the leading term of equation (2) is minimized when $\mathbf{M} = \Gamma^{-1}$[16].

In FAMIS, when applying the fixed effect model to the transformed trixels y_i, the effect $\tilde{y}_i$ represents the relevant part of the trixel y_i, while the noise is assumed to be the random error σe_i. $\mathbb{S}$ is the subspace which corresponds to the so called study subspace[17], in which the relevant part of the trixels is properly restored, without the noise. So, the optimal study space $\mathbb{S}$ can be computed if Γ is known or can be estimated.

Application to scintigraphic data

When processing radionuclide image sequences, a trixel x_i is the realization of P Poisson distributed variables of parameters v_{ij}. The best first order approximation of v_{ij} is $v_{ij} = \frac{v_{i.}v_{.j}}{v_{..}}$[18] where $v_{i.} = \sum_{j=1}^{P} v_{ij}$, $v_{.j} = \sum_{i=1}^{N} v_{ij}$ and $v_{..} = \sum_{i=1}^{N}\sum_{j=1}^{P} v_{ij}$. $v_{i.}$, $v_{.j}$ and $v_{..}$ are unknown, but can be replaced by their maximum likelihood estimators $x_{i.}$, $x_{.j}$ and $x_{..}$ with $x_{i.} = \sum_{j=1}^{P} x_{ij}$, $x_{.j} = \sum_{i=1}^{N} x_{ij}$ and $x_{..} = \sum_{i=1}^{N}\sum_{j=1}^{P} x_{ij}$.

To analyse the shape of the trixels, we consider in FAMIS the transformation $y_i = g(x_i) = \frac{1}{x_{i.}} x_i$. It follows that:

$$E(y_i) = \frac{1}{x_{i.}} E(x_i) = \left(\frac{x_{.1}}{x_{..}}, \ldots, \frac{x_{.j}}{x_{..}}, \ldots, \frac{x_{.P}}{x_{..}} \right) \text{ and:}$$

$$\mathrm{Var}(y_i) = \frac{1}{x_{i.}^2} \mathrm{Var}(x_i) = \mathrm{diag}\left(\frac{x_{.1}}{x_{i.}x_{..}}, \ldots, \frac{x_{.j}}{x_{i.}x_{..}}, \ldots, \frac{x_{.P}}{x_{i.}x_{..}} \right)$$

In comparison with expression (1) of the variance given by the fixed effect model, and for σ^2 to be small, the following identifications are performed:

$$\sigma^2 = \frac{1}{x_{..}}, \quad \omega_i = \frac{x_{i.}}{x_{..}} \quad \text{and}$$

$$\Gamma = \mathrm{diag}\left(\frac{x_{.1}}{x_{..}}, \ldots, \frac{x_{.j}}{x_{..}}, \ldots, \frac{x_{.P}}{x_{..}} \right)$$

Then, according to the solution of the fixed effect model, $\mathbb{S}$ contains $\bar{y}$ with:

$$\bar{y}(j) = \frac{1}{\sum_{i=1}^{N} \omega_i} \sum_{i=1}^{N} \omega_i y_i(j) = \sum_{i=1}^{N} \frac{x_{i.}x_{ij}}{x_{..}x_{i.}} = \frac{x_{.j}}{x_{..}}$$

$\mathbb{S}$ is spanned by the Q eigenvectors φ_q associated with the Q largest eigenvalues λ_q of the matrix:

$$(\mathbf{Y} - 1_N \bar{\mathbf{Y}})' \mathbf{W} (\mathbf{Y} - 1_N \bar{\mathbf{Y}}) \mathbf{M},$$

$$\text{with } \bar{\mathbf{Y}} = \left(\frac{x_{.1}}{x_{..}}, \ldots, \frac{x_{.j}}{x_{..}}, \ldots, \frac{x_{.P}}{x_{..}} \right)$$

$$\mathbf{W} = \mathrm{diag}\left(\frac{x_{1.}}{x_{..}}, \ldots, \frac{x_{i.}}{x_{..}}, \ldots, \frac{x_{N.}}{x_{..}} \right),$$

$$\mathbf{M} = \Gamma^{-1} = \mathrm{diag}\left(\frac{x_{..}}{x_{.1}}, \ldots, \frac{x_{..}}{x_{.j}}, \ldots, \frac{x_{..}}{x_{.P}} \right)$$

The eigendecomposition of this matrix corresponds to the eigendecomposition of correspondence analysis (CA)[19]. Consequently, the optimal orthogonal decomposition to determine the study space for scintigraphic data is the one of correspondence analysis[20].

In CA, the relevant part of the trixels, $\tilde{x}_i$, can be reconstituted using the following reconstitution formula[19]:

$$\mathbf{D}_\mathbf{N}^{-1} \mathbf{X} \mathbf{D}_\mathbf{P}^{-1} = 1_\mathbf{N} 1_\mathbf{P}' + \psi_\mathbf{Q}' \Lambda_\mathbf{Q}^{-1/2} \varphi_\mathbf{Q} = \psi' \Lambda^{-1/2} \varphi \qquad (3)$$

where $\mathbf{X}$ is the (N, P) matrix of elements $\frac{x_{ij}}{x_{..}}$, $\mathbf{D}_\mathbf{N}$ is the (N, N) diagonal matrix of $\frac{x_{i.}}{x_{..}}$, $\mathbf{D}_\mathbf{P}$ is the (P, P) diagonal matrix of $\frac{x_{.j}}{x_{..}}$, and:

$$\psi = \begin{pmatrix} 1 & \ldots & 1 \\ & \psi_\mathbf{Q} & \end{pmatrix}, \quad \varphi = \begin{pmatrix} 1 & \ldots & 1 \\ & \varphi_\mathbf{Q} & \end{pmatrix},$$

$$\text{and} \quad \Lambda = \begin{pmatrix} 1 & 0 \\ 0 & \Lambda_\mathbf{Q} \end{pmatrix}$$

$\varphi_\mathbf{Q}$ is the (Q, P) matrix of the eigenvectors φ_q. $\psi_\mathbf{Q}$ is the (Q, N) matrix of vectors ψ_q such that $\psi_\mathbf{Q} = \Lambda_\mathbf{Q}^{-1/2} \varphi_\mathbf{Q} \mathbf{X}' \mathbf{D}_\mathbf{N}^{-1}$. $\Lambda_\mathbf{Q}$ is the (Q, Q) diagonal matrix whose diagonal elements are equal to the eigenvalues λ_q. Furthermore, we have $\psi_\mathbf{Q} \mathbf{D}_\mathbf{N} \psi_\mathbf{Q}' = \Lambda_\mathbf{Q}$:

$$\psi_\mathbf{Q} \mathbf{D}_\mathbf{N} 1_\mathbf{N} = 0 \qquad (4)$$

$$\text{and} \quad 1_\mathbf{N}' \mathbf{D}_\mathbf{N} 1_\mathbf{N} = 1 \qquad (5)$$

hence:

$$\psi \mathbf{D}_\mathbf{N} \psi' = \Lambda \qquad (6)$$

Symmetrically, we also have $\varphi_\mathbf{Q} \mathbf{D}_\mathbf{P} \varphi_\mathbf{Q}' = \Lambda_\mathbf{Q}$:

$$\varphi_\mathbf{Q} \mathbf{D}_\mathbf{P} 1_\mathbf{P} = 0 \qquad (7)$$

and:

$$\varphi \mathbf{D}_\mathbf{P} \varphi' = \Lambda \qquad (8)$$

Thus:

$$\varphi \mathbf{D}_\mathbf{P} \varphi' = \Lambda \qquad (9)$$

In what follows, we deal with the case of the study space obtained by CA.

FAMIS PHYSICAL MODEL IN A UNIFIED METHOD OF OBLIQUE ANALYSIS

The relevant part of trixels obtained by the solution of the statistical model is assumed to follow a physical model.

Physical model

The physical model of FAMIS states that the relevant part of each trixel x_i can be expressed as a linear combination of a limited number K of fundamental functions f_k, weighted by coefficients $a_k(i)$ depending on i. We write this model as:

$$\frac{1}{x_{..}} \tilde{x}_{ij} = \sum_{k=1}^{K} \frac{1}{K} a_k(i) f_k(j), \quad \text{i.e. } \mathbf{X} = \frac{1}{K} \mathbf{A}' \mathbf{F} \qquad (10)$$

where $\mathbf{F}$ is the (K, P) matrix of the fundamental functions and $\mathbf{A}$ is the (K, N) matrix of the fundamental spatial distributions.

This model can be read symmetrically: the relevant part of each image x_j of the sequence is a linear combination of the fundamental spatial distributions a_k, weighted by coefficients $f_k(j)$.

FAMIS assumes that the number K of fundamental

structures is equal to the dimension of the study space, i.e. $K = Q + 1$ ($\bar{y}$ and Q eigenvectors).

Two symmetrical hypotheses can be considered for solving the physical model:

- on the one hand, a hypothesis related to the fundamental functions, deduced from the conventional hypothesis[1];
- on the other hand, a hypothesis related to the fundamental spatial distributions.

The fundamental functions and spatial distributions are estimated by factors and factor images, respectively.

Hypothesis related to the fundamental functions

The orthogonal analysis states that the relevant part of any trixel $\frac{\tilde{x}_i}{x_{i.}}$ is represented in the study space $\mathbb{S}$, including $\bar{y}$ and spanned by the vectors φ_q (equation (3)):

$$\frac{\tilde{x}_{ij}}{x_{i.}} = \frac{x_{.j}}{x_{..}} + \sum_{q=1}^{Q} \frac{\psi_q(i)}{\sqrt{\lambda_q}} \frac{x_{.j}}{x_{..}} \varphi_q(j)$$

Hypothesis 1 considers that the fundamental functions belong to $\mathbb{S}$:

$$f_k(j) = \frac{x_{.j}}{x_{..}} + \sum_{q=1}^{Q} \beta_{kq} \frac{x_{.j}}{x_{..}} \varphi_q(j)$$

i.e. in matrix notation:

$$\mathbf{F} = 1_{\mathbf{K}}\, 1_{\mathbf{P}}' \mathbf{D}_{\mathbf{P}} + \beta_{\mathbf{Q}}\, \varphi_{\mathbf{Q}}\, \mathbf{D}_{\mathbf{P}} = \beta\, \varphi\, \mathbf{D}_{\mathbf{P}} \tag{11}$$

where $\beta_{\mathbf{Q}}$ is the (K, Q) matrix of elements β_{kq} and:

$$\beta = \begin{pmatrix} 1 & \\ \vdots & \beta_{\mathbf{Q}} \\ 1 & \end{pmatrix}$$

A factor f_k is so determined by the point $\{\beta_{kq}\}_{q=1,\ldots,Q}$, also called pole k.

By multiplying equation (11) on the right by φ^t, then using equation (9), we obtain:

$$\mathbf{F}\, \varphi^t = \beta\, \varphi\, \mathbf{D}_{\mathbf{P}}\, \varphi^t = \beta\, \Lambda$$

Therefore, if $\mathbf{F}$ is known, β can be deduced from $\mathbf{F}$ by:

$$\beta = \mathbf{F}\, \varphi^t\, \Lambda^{-1} \tag{12}$$

By multiplying equation (11) on the right by $1_{\mathbf{P}}$, we get $\mathbf{F}\, 1_{\mathbf{P}} = 1_{\mathbf{K}}\, 1_{\mathbf{P}}\, \mathbf{D}_{\mathbf{P}}\, 1_{\mathbf{P}} + \beta_{\mathbf{Q}}\, \varphi_{\mathbf{Q}}\, \mathbf{D}_{\mathbf{P}}\, 1_{\mathbf{P}} = 1_{\mathbf{K}}$, due to equations (7) and (8).

Consequently, hypothesis 1 combined with CA decomposition leads to the factor normalization:

$$\mathbf{F}\, 1_{\mathbf{P}} = 1_{\mathbf{K}} \tag{13}$$

This normalization yields a normalization for the factor images. Indeed:

$$\begin{aligned} \mathbf{D}_{\mathbf{N}}^{-1}\, \mathbf{X}\, \mathbf{D}_{\mathbf{P}}^{-1}\, \mathbf{D}_{\mathbf{P}}\, 1_{\mathbf{P}} &= \mathbf{D}_{\mathbf{N}}^{-1}\, \mathbf{X}\, (\mathbf{D}_{\mathbf{P}}^{-1}\, \mathbf{D}_{\mathbf{P}})\, 1_{\mathbf{P}} \\ &= \mathbf{D}_{\mathbf{N}}^{-1}\, (\mathbf{X}\, 1_{\mathbf{P}}) = 1_{\mathbf{N}} \end{aligned}$$

that is, using equation (10):

$$\frac{1}{K}\, \mathbf{D}_{\mathbf{N}}^{-1}\, \mathbf{A}^t\, \mathbf{F}\, 1_{\mathbf{P}} = 1_{\mathbf{N}}$$

By substituting $1_{\mathbf{K}}$ for $\mathbf{F}\, 1_{\mathbf{P}}$, the normalization for the factor images follows:

$$\frac{1}{K}\, \mathbf{D}_{\mathbf{N}}^{-1}\, \mathbf{A}^t\, 1_{\mathbf{K}} = 1_{\mathbf{N}} \tag{14}$$

Let us introduce hypothesis 1 into the physical decomposition of FAMIS. From equations (10) and (11) we get:

$$\begin{aligned} \mathbf{D}_{\mathbf{N}}^{-1}\, \mathbf{X}\, \mathbf{D}_{\mathbf{P}}^{-1} &= \frac{1}{K}\, \mathbf{D}_{\mathbf{N}}^{-1}\, \mathbf{A}^t\, \mathbf{F}\, \mathbf{D}_{\mathbf{P}}^{-1} \\ &= \frac{1}{K}\, \mathbf{D}_{\mathbf{N}}^{-1}\, \mathbf{A}^t\, [1_{\mathbf{K}}\, 1_{\mathbf{P}}'\, \mathbf{D}_{\mathbf{P}} + \beta_{\mathbf{Q}}\, \varphi_{\mathbf{Q}}\, \mathbf{D}_{\mathbf{P}}]\, \mathbf{D}_{\mathbf{P}}^{-1} \\ &= \frac{1}{K}\, \mathbf{D}_{\mathbf{N}}^{-1}\, \mathbf{A}^t\, 1_{\mathbf{K}}\, 1_{\mathbf{P}}' + \frac{1}{K}\, \mathbf{D}_{\mathbf{N}}^{-1}\, \mathbf{A}^t\, \beta_{\mathbf{Q}}\, \varphi_{\mathbf{Q}} \end{aligned}$$

Using equation (14), this can be written as:

$$\mathbf{D}_{\mathbf{N}}^{-1}\, \mathbf{X}\, \mathbf{D}_{\mathbf{P}}^{-1} = 1_{\mathbf{N}}\, 1_{\mathbf{P}}' + \frac{1}{K}\, \mathbf{D}_{\mathbf{N}}^{-1}\, \mathbf{A}^t\, \beta_{\mathbf{Q}}\, \varphi_{\mathbf{Q}} \tag{15}$$

By identifying equations (3) and (15), it follows that:

$$\frac{1}{K}\, \mathbf{D}_{\mathbf{N}}^{-1}\, \mathbf{A}^t\, \beta_{\mathbf{Q}} = \psi_{\mathbf{Q}}'\, \Lambda_{\mathbf{Q}}^{-1/2} \tag{16}$$

Equations (14) and (16) can be rewritten in a single equation:

$$\frac{1}{K}\, \mathbf{D}_{\mathbf{N}}^{-1}\, \mathbf{A}^t\, \beta = \psi^t\, \Lambda^{-1/2}$$

To summarize:

- CA and hypothesis 1 imply the factor normalization $\mathbf{F}\, 1_{\mathbf{P}} = 1_{\mathbf{K}}$, which is no longer an arbitrary one[1,3].
- CA, physical model and hypothesis 1 give the image factor normalization $\frac{1}{K}\, \mathbf{D}_{\mathbf{N}}^{-1}\, \mathbf{A}^t\, 1_{\mathbf{K}} = 1_{\mathbf{N}}$ and the relationship $\frac{1}{K}\, \mathbf{D}_{\mathbf{N}}^{-1}\, \mathbf{A}^t\, \beta = \psi^t\, \Lambda^{-1/2}$.

Hypothesis related to the fundamental spatial distributions

In dual fashion, the orthogonal analysis states that the relevant part of any normalized image, $\frac{\tilde{x}_j}{x_{.j}}$, is represented in a space $\mathbb{S}^*$, containing $\frac{x_{i.}}{x_{..}}$ and spanned by the ψ_q (equation (3)):

$$\frac{x_{ij}}{x_{.j}} = \frac{x_{i.}}{x_{..}} + \sum_{q=1}^{Q} \varphi_q(j) \frac{x_{i.}}{x_{..}} \frac{\psi_q(i)}{\sqrt{\lambda_q}}$$

Hypothesis 2 considers that the fundamental spatial distributions belong to $\mathbb{S}^*$:

$$a_k(i) = \frac{x_{i.}}{x_{..}} + \sum_{q=1}^{Q} \gamma_{kq} \frac{x_{i.}}{x_{..}} \frac{\psi_q(i)}{\sqrt{\lambda_q}}$$

i.e. in matrix notation:

$$\mathbf{A} = 1_K 1_N^t \mathbf{D}_N + \gamma_Q \Lambda_Q^{1/2} \psi_Q \mathbf{D}_N = \gamma \Lambda^{1/2} \psi \mathbf{D}_N \quad (17)$$

where γ_Q is the (K, Q) matrix of elements γ_{kq} and:

$$\gamma = \begin{pmatrix} 1 & & \\ \vdots & \gamma_Q & \\ 1 & & \end{pmatrix}$$

A factor image a_k is thus defined by the location of its image pole γ_k in the image space $\mathbb{S}^*$.

By multiplying equation (17) on the right by ψ^t, then using equation (6), we get:

$$\mathbf{A} \psi^t = \gamma \Lambda^{1/2} \psi \mathbf{D}_N \psi^t = \gamma \Lambda^{1/2}$$

When $\mathbf{A}$ is known, γ can then be deduced from $\mathbf{A}$ by:

$$\gamma = \mathbf{A} \psi^t \Lambda^{-1/2} \quad (18)$$

Multiplying equation (17) on the right by 1_N and using equations (4) and (5) yields:

$$\mathbf{A} 1_N = 1_K 1_N^t \mathbf{D}_N 1_N + \gamma_Q \Lambda_Q^{1/2} \psi_Q \mathbf{D}_N 1_N = 1_K$$

In other words, hypothesis 2 and CA decomposition involve the factor image normalization:

$$\mathbf{A} 1_N = 1_K \quad (19)$$

As $\mathbf{D}_P^{-1} \mathbf{X}^t \mathbf{D}_N^{-1} \mathbf{D}_N 1_N = \mathbf{D}_P^{-1} \mathbf{X}^t (\mathbf{D}_N^{-1} \mathbf{D}_N)$

$1_N = \mathbf{D}_P^{-1} (\mathbf{X}^t 1_N) = 1_P$, by introducing the physical model (10) into this relationship, we get:

$$\frac{1}{K} \mathbf{D}_P^{-1} \mathbf{F}^t \mathbf{A} 1_N = 1_P$$

If we replace $\mathbf{A} 1_N$ by 1_K (19), we obtain the following normalization for the factors:

$$\frac{1}{K} \mathbf{D}_P^{-1} \mathbf{F}^t 1_K = 1_P \quad (20)$$

Let us now combine physical model (10) and hypothesis 2 (17). This yields:

$$\mathbf{D}_N^{-1} \mathbf{X} \mathbf{D}_P^{-1} = \frac{1}{K} \mathbf{D}_N^{-1} \mathbf{A}^t \mathbf{F} \mathbf{D}_P^{-1}$$

$$= \frac{1}{K} \mathbf{D}_N^{-1} [\mathbf{D}_N 1_N 1_K^t + \mathbf{D}_N \psi_Q^t \Lambda_Q^{-1/2} \gamma_Q^t] \mathbf{F} \mathbf{D}_P^{-1}$$

$$= \frac{1}{K} 1_N 1_K^t \mathbf{F} \mathbf{D}_P^{-1} + \frac{1}{K} \psi_Q^t \Lambda_Q^{1/2} \gamma_Q^t \mathbf{F} \mathbf{D}_P^{-1}$$

Using the transpose of the relationship (20), we have:

$$\mathbf{D}_N^{-1} \mathbf{X} \mathbf{D}_P^{-1} = 1_N 1_P^t + \frac{1}{K} \psi_Q^t \Lambda_Q^{1/2} \gamma_Q^t \mathbf{F} \mathbf{D}_P^{-1}$$

By identifying this expression with CA decomposition (3), we get:

$$\varphi_Q = \frac{1}{K} \gamma_Q^t \mathbf{F} \mathbf{D}_P^{-1} \quad (21)$$

Equations (20) and (21) are associated in a single equation:

$$\varphi = \frac{1}{K} \gamma^t \mathbf{F} \mathbf{D}_P^{-1} \quad (22)$$

To sum up:

- CA and hypothesis 2 imply the factor image normalization $\mathbf{A} 1_N = 1_K$.
- CA, physical model and hypothesis 2 give the factor normalization $\frac{1}{K} \mathbf{D}_P^{-1} \mathbf{F}^t 1_K = 1_P$ and the relationship $\frac{1}{K} \gamma^t \mathbf{F} \mathbf{D}_P^{-1} = \varphi$.

Mixture of the two hypotheses

From hypothesis 1, equation (14) follows. By multiplying on the left by $1_N^t \mathbf{D}_N$ and on the right by 1_K^t, we obtain $1_N^t \mathbf{A}^t = 1_K^t$, i.e. the normalization (19) resulting from hypothesis 2.

Conversely, hypothesis 2 yields the relationships (20). By multiplying on the left by $1_P^t \mathbf{D}_P$ and on the right by 1_K^t, we get $1_P^t \mathbf{F}^t = 1_K^t$, that is the normalization (13) resulting from hypothesis 1.

This proves that hypotheses 1 and 2 are compatible. Consequently, they can be mixed to derive relationships for solving the physical model without being in favour of one particular hypothesis.

By using relationships issued from CA (4), hypothesis 1 (16) and hypothesis 2 (19), we get:

$$\psi_Q \mathbf{D}_N 1_N = 0 = \frac{1}{K} \Lambda_Q^{1/2} \beta_Q^t \mathbf{A} \mathbf{D}_N^{-1} \mathbf{D}_N 1_N$$

$$= \frac{1}{K} \Lambda_Q^{1/2} \beta_Q^t 1_K$$

Hence, $\beta_Q^t 1_K = 0 \quad (23)$

Similarly, by associating results issued from CA (7), hypothesis 2 (21) and hypothesis 1 (13), we obtain:

$$\varphi_Q \mathbf{D}_P 1_P = 0 = \frac{1}{K} \gamma_Q^t \mathbf{F} \mathbf{D}_P^{-1} \mathbf{D}_P 1_P$$

$$= \frac{1}{K} \gamma_Q^t \mathbf{F} 1_P \quad \frac{1}{K} \gamma_Q^t 1_K$$

then:

$$\gamma_Q^t 1_K = 0 \quad (24)$$

By combining hypothesis 1 (11) and the result issued from hypothesis 2 (22), it follows that $\mathbf{F} \mathbf{D}_P^{-1} = \beta \varphi = \frac{1}{K} \beta \gamma^t \mathbf{F} \mathbf{D}_P^{-1}$. Consequently:

$$\frac{1}{K} \beta \gamma^t = \mathbf{Id} \quad (25)$$

where $\mathbf{Id}$ is the identity matrix. From this relationship, the coefficients β_{kq} leading to the factors can be computed from the coefficients γ_{kq}, and conversely.

Solution to the physical model by joint use of the hypotheses

The physical model is solved by means of an iterative procedure (*Figure 1*), which runs using:

(i) relationships deduced from hypothesis 1, hypothesis 2, and mixture of both hypotheses;
(ii) constraints derived from *a priori* knowledge:
- in all cases, non-negativity constraints derived from the non-negativity of the fundamental functions and spatial distributions, which is essential for them to have a physical or physiological meaning;
- optionally, fixed pole and/or fixed image pole constraints. They result from the known locations in $\mathbb{S}$ or $\mathbb{S}^*$ of some fundamental functions and/or spatial distributions. These locations are determined before the iterative procedure, for instance by means of a target apex seeking[21].

The iterative procedure is initialized from a first estimate of β (step 1 of the algorithm in *Figure 1*) or from a first estimate of γ. In this latter case, it begins at step 8. The commonly used initialization[3] which takes place in the function space $\mathbb{S}$ can be adapted to the initialization of γ in the image space $\mathbb{S}^*$ as follows:

- the first image pole is the point $\{\varphi_q(j)\}\, q = 1, \ldots, Q$ which is the most distant from the origin;
- the second image pole is the point $\{\varphi_q(j)\}\, q = 1, \ldots, Q$ furthest from the first image pole;
- ...
- the Kth image pole is the point $\{\varphi_q(j)\}\, q = 1, \ldots, Q$ for which the sum of the distances to the $(K-1)$ other image poles is maximum.

The iterative procedure then runs according to the algorithm in *Figure 1*: for instance, when starting with a first estimate of the matrix β, such that $\beta'_{\mathbf{Q}}\, 1_{\mathbf{K}} = 0$ (23), the corresponding factors are computed from equation (11). Non-negativity constraints related to the fundamental functions are applied to modify the values of f_k. The resulting $\mathbf{F}$ is normalized to verify $\mathbf{F}\, 1_{\mathbf{P}} = 1_{\mathbf{K}}$ (13), and the corresponding β is computed using equation (12). The *a priori* known poles are replaced by their fixed values. The new value of γ is computed from equation (25), as the associated factor images using equation (17). Non-negativity constraints related to the fundamental spatial distributions are then applied to the $a_k(i)$. $\mathbf{A}$ is normalized, such that $\mathbf{A}\, 1_{\mathbf{N}} = 1_{\mathbf{K}}$ (19), and the corresponding γ is computed by equation (18). Fixed image poles are restored. The corresponding β is calculated from equation (25), and this value of β is used to start a new iteration.

The iterative procedure is repeated until one stopping criterion is satisfied, for instance, when the number of negative values of $f_k(j)$ or $a_k(i)$ is low enough. The stopping criteria are assessed at the end of steps 7 and 13 and, when a stopping criterion is satisfied, β and γ are known.

FAMIS can be performed on data issued from a spatial sampling different from the initial spatial sampling of the image sequence[3]. The factor images in the initial spatial sampling are then computed by an oblique projection of the image sequence onto the factors corresponding to β[3].

1 Estimation of the poles β.

2 Computation of the associated factors $\mathbf{F}$ from $\mathbf{F} = \beta\, \varphi\, \mathbf{D_P}$ (equation (11)).

3 Modification of the factors $\mathbf{F}$ using non-negativity constraints:
if $f_k(j) < 0, f_k(j)$ is replaced by 0.

4 Normalization of the factors $\mathbf{F}$, such that $\mathbf{F}\, 1_{\mathbf{P}} = 1_{\mathbf{K}}$ (equation (13)).

5 Computation of the associated poles β by $\beta = \mathbf{F}\, \varphi'\, \Lambda^{-1}$ (equation (12)).

6 Restoration of some fixed poles.

7 Computation of the corresponding image poles γ by $\gamma' = K\beta^{-1}$ (equation (25)).

8 Computation of the associated factor images $\mathbf{A}$ from $\mathbf{A} = \gamma\, \Lambda^{-1/2}\, \psi\, \mathbf{D_N}$ (equation (17)).

9 Modification of the factor images $\mathbf{A}$ using non-negativity constraints:
if $a_k(i) < 0$, $a_k(i)$ is replaced by 0.

10 Normalization of the factor images $\mathbf{A}$ such that $\mathbf{A}\, 1_{\mathbf{N}} = 1_{\mathbf{K}}$ (equation (19)).

11 Computation of the corresponding image poles γ by $\gamma = \mathbf{A}\, \psi'\, \Lambda^{-1/2}$ (equation (18)).

12 Restoration of some fixed image poles.

13 Computation of the corresponding poles β by $\beta' = K\gamma^{-1}$ (equation (25)).

14 Return to step 2.

Figure 1 Algorithm of oblique analysis

EXAMPLES

Importance of oblique analysis initialization

Method

A computer-simulated phantom is used to compare FAMIS results according to the space in which the first estimation of the fundamental structures is performed. It consists of three rectangular overlapping spatial distributions a_1, a_2 and a_3 associated with three fundamental functions f_1, f_2 and f_3 (*Figure 2*). The contributions Contr(k) of each fundamental structure k, defined by:

$$\mathrm{Contr}(k) = \frac{\sum_{m=1}^{M} c_k(m)}{\sum_{k=1}^{K} \left[\sum_{m=1}^{M} c_k(m) \right]}$$

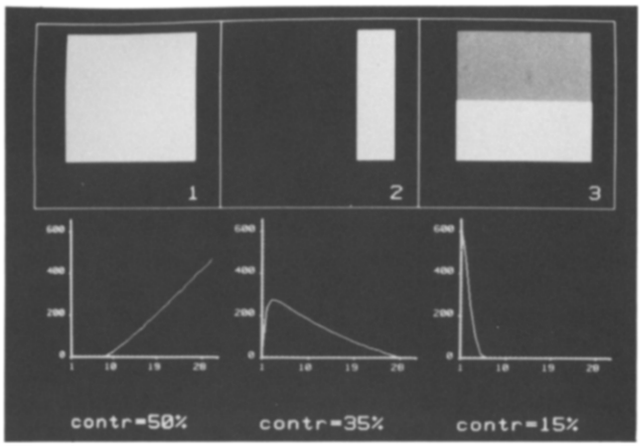

Figure 2 Three fundamental structures of the computer-simulated phantom and associated contributions

$$\text{with} \quad \begin{cases} c_k(m) = a_k(i) & \text{and } M = N \text{ if } \mathbf{F}\,1_{\mathbf{P}} = 1_{\mathbf{K}} \\ c_k(m) = f_k(j) & \text{and } M = P \text{ if } \mathbf{A}\,1_{\mathbf{N}} = 1_{\mathbf{K}} \end{cases}$$

are 50%, 35% and 15%, respectively. A sequence of 30 images 64 × 64 is computed from:

$$x_{ij} = \sum_{k=1}^{K} a_k(i) f_k(j)$$

and Poisson noise is added.

The resulting sequence is first preprocessed: the contents of neighbouring trixels are summed according to a 4 × 4 pattern. All the trixels different from zero are submitted to the orthogonal decomposition of CA, followed by the oblique analysis (as has been previously described) using only the non-negativity constraints related to the fundamental functions and spatial distributions. In the oblique analysis, two initializations are tested:

- initialization of the poles in the function space $\mathbb{S}$: a first estimate of β is obtained from the location of the trixels in this space. The iterative procedure starts from step 2 of the algorithm;
- initialization of the image poles in the image space $\mathbb{S}^*$: γ is first estimated using the location of the images in this space. The iterations then begin from step 8.

Results

Initialization in $\mathbb{S}$: *Figure 3* shows the distribution of the 121 trixels in $\mathbb{S}$ and that of the 30 images in $\mathbb{S}^*$. The locations of final poles and image poles within each of these spaces are also displayed. As the initialization takes place in $\mathbb{S}$, the final poles (i.e. β) satisfying the non-negativity constraints are the apices of the tightest triangle including all the trixels projections in $\mathbb{S}^1$. In $\mathbb{S}^*$, the apices of the corresponding triangle are the image poles (i.e. γ), which define a large triangle, since $1\mathbf{K}\,\beta\,\gamma^t = \mathbf{Id}$ (equation (25)). Apex 3 of the pole triangle corresponds to a trixel described by several fundamental functions, since there is no trixel described by only fundamental function f_3 in the simulated data. f_3 is thus a poor estimation of f_3. Apex 1 is also at a wrong position in $\mathbb{S}$. Consequently, factors, factor images and estimated contributions are erroneous (*Figure 4*).

Initialization in $\mathbb{S}^*$: in a dual fashion, when the initialization is performed in $\mathbb{S}^*$, the final image poles (i.e. γ) satisfying the non-negativity constraints are the apices of the smallest triangle containing all the projections of the images (*Figure 5*). The corresponding triangle in $\mathbb{S}$ is a large one, far from the cloud of trixel projections. Due to the initialization procedure, the apices of the image pole triangle correspond to images in which only one fundamental structure is present (images 1, 7 and 30). Consequently, the final factor images are quite correct, as are the associated factors and contributions (*Figure 6*).

Joint use of *a priori* knowledge related to the fundamental functions and spatial distributions

Method

We illustrate the interest of the joint use of *a priori* knowledge related to both fundamental functions and

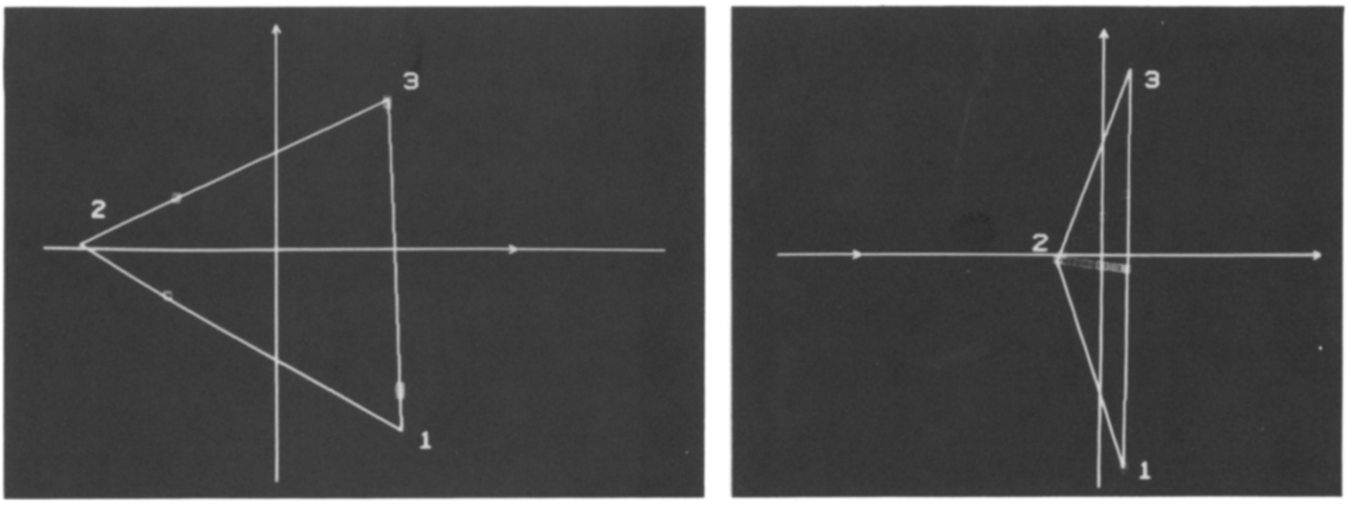

Figure 3 After initialization in the function space $\mathbb{S}$. (Left) Trixel projections (□) in $\mathbb{S}$ and final location of the poles β_1 (1), β_2 (2) and β_3 (3); (right) image projections (□) in $\mathbb{S}^*$ and final location of the poles γ_1 (1), γ_2 (2) and γ_3 (3)

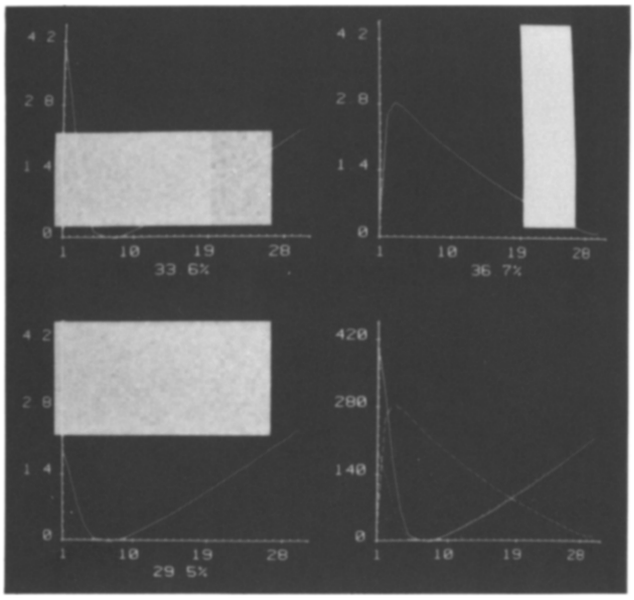

Figure 4 After initialization in the function space $\mathbb{S}$: final estimation of the fundamental structures and associated contributions. *a* (top left): $(\hat{a}_3, \hat{f}_3)$, *b* (top right): $(\hat{a}_2, \hat{f}_2)$, *c* (bottom left): $(\hat{a}_1, \hat{f}_1)$, *d* (bottom right): superimposition of the three factors

spatial distributions for FAMIS to give a good estimate of the fundamental structures. A computer-simulated phantom is made up of three rectangular spatial distributions associated with three functions, with contributions equal to 20%, 40% and 40%, respectively (*Figure 7*). An image sequence is computed from these structures and Poisson noise is added. The resulting sequence is submitted to three FAMIS. Each one processes all the trixels different from zero (i.e. 121 trixels) obtained after 4 × 4 spatial sampling, and begins with the orthogonal decomposition of CA. The three FAMIS differ by the *a priori* knowledge taken into account besides the non-negativity, and by the space used for the initialization:

- FAMIS 1: a factor $\hat{f}_1$ is determined by a target apex seeking procedure[21] knowing that one fundamental function becomes zero from image 17. The criterion minimized during the search is defined by:

$$h(s) = \sum_{j=17}^{30} s^2(j)$$

where s is the curve associated with any point (β_1, β_2) of the function space $\mathbb{S}$:

$$s(j) = \frac{x_{.j}}{x_{..}} + \sum_{q=1}^{2} \beta_q \frac{x_{.j}}{x_{..}} \varphi_q(j)$$

The other factors are initialized in $\mathbb{S}$ using the conventional procedure[3], with the first pole corresponding to $\hat{f}_1$.

This fixed factor $\hat{f}_1$ is restored at each iteration (step 6 of the algorithm) of the oblique analysis.

FAMIS 2: an homogeneous background factor image, corresponding to a_2, is searched for in the image space $\mathbb{S}$ by a target apex seeking procedure, similar to the one used when seeking for factors[21]. The criterion to minimize is now:

$$h(r) = \sum_{i=1}^{121} \left(r(i) - \frac{1}{121} \right)^2$$

where 121 is the number of processed trixels and r is the image associated with any point (γ_1, γ_2) of $\mathbb{S}^*$:

$$r(i) = \frac{x_{i.}}{x_{..}} + \sum_{q=1}^{2} \gamma_q \frac{x_{i.}}{x_{..}} \frac{\psi_q(i)}{\sqrt{\lambda_q}}$$

Other *a priori* knowledge is that the 30th image corresponds to one fundamental spatial distribution, a_3, and is therefore taken as a factor image. The third factor image is initialized in $\mathbb{S}^*$, as described earlier, after the localization of the two other image poles.

Two factor images ($\hat{a}_2$ and $\hat{a}_3$) are restored at each iteration (step 12 of the algorithm) during the oblique analysis.

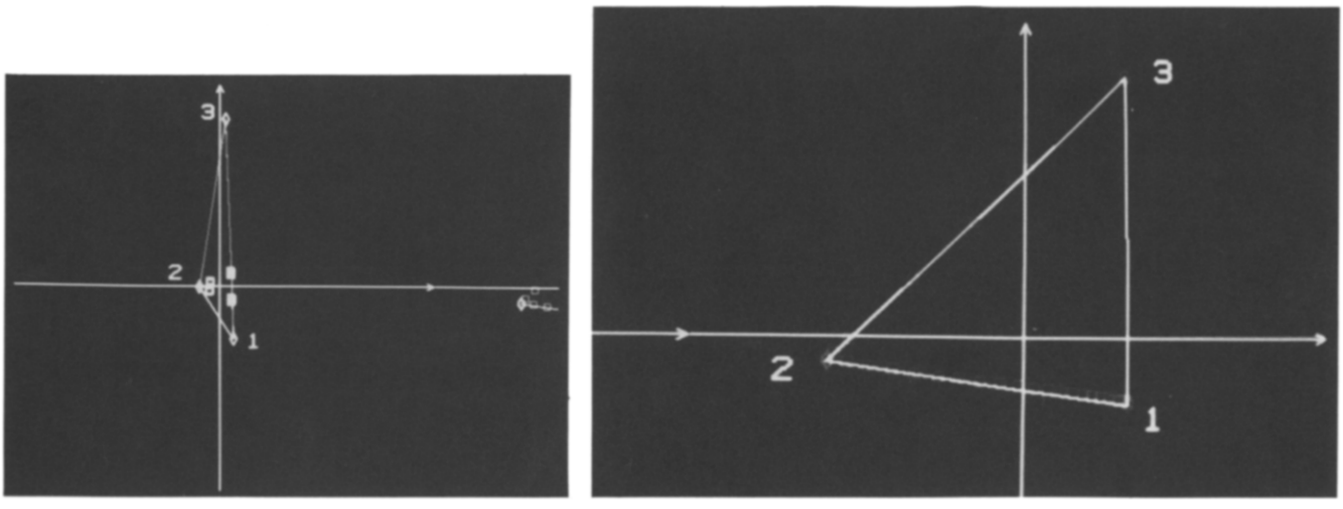

Figure 5 After initialization in the image space $\mathbb{S}^*$. (Left) Trixel projections (□) in $\mathbb{S}$ and final location of the poles β_1 (1), β_2 (2) and β_3 (3); (right) image projections (□) in $\mathbb{S}^*$ and final location of the poles γ_1 (1), γ_2 (2) and γ_3 (3)

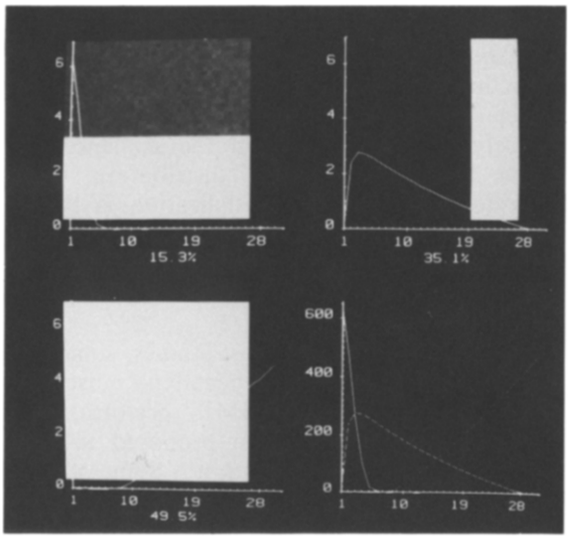

Figure 6 After initialization in the image space $\mathbb{S}$: final estimation of the fundamental structures and associated contributions. *a* (top left): $(\hat{a}_3, \hat{f}_3)$, *b* (top right): $(\hat{a}_2, \hat{f}_2)$, *c* (bottom left): $(\hat{a}_1, \hat{f}_1)$, *d* (bottom right): superimposition of the three factors

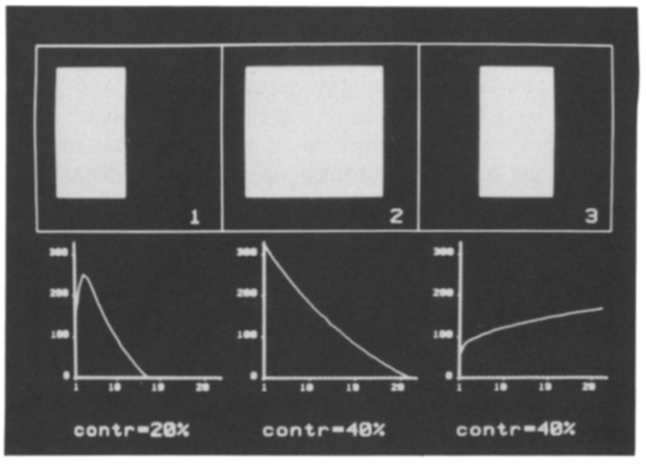

Figure 7 Three fundamental structures of the computer-simulated phantom and associated contributions

- FAMIS 3: the initialization is performed as in FAMIS 1, that is the first factor $\hat{f}_1$ is searched for by the target apex seeking procedure, and the first estimation of the two others takes place in $\mathbb{S}$. $\hat{a}_2$ and $\hat{a}_3$ are determined as in FAMIS 2. At each iteration of the oblique analysis, $\hat{f}_1$, $\hat{a}_2$ and $\hat{a}_3$ are restored.

Results

FAMIS 1 and FAMIS 2 lead to poor estimate of the fundamental structures and contributions (*Figures 8* and *9*). In FAMIS 1, the target apex seeking correctly finds f_1. $\hat{f}_2$ is a suitable estimate of f_2 since there are some trixels described by the single function f_2 among the set of trixels. However, there is no trixel described by the only function f_3 and FAMIS fails at estimating this function (*Figure 8*). In FAMIS 2, a_2 and a_3 are properly estimated thanks to the *a priori* knowledge. $\hat{a}_1$ deviates substantially from a_1 (*Figure 9*), in particular because of the lack of images including the single spatial distribution a_1 in the initial image sequence.

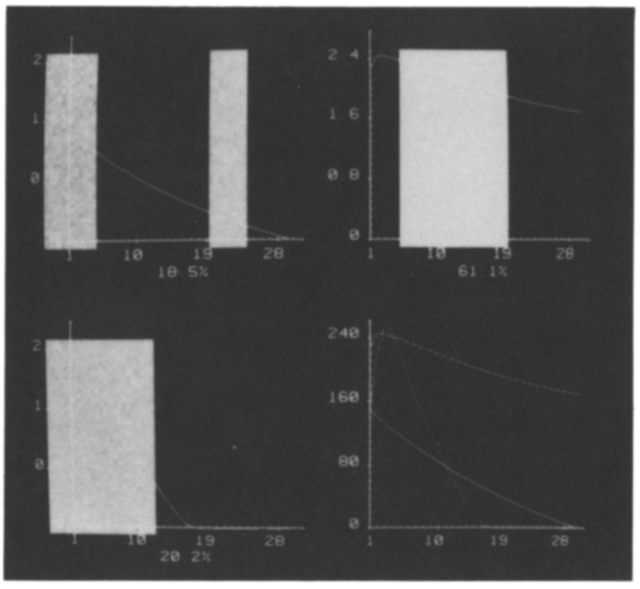

Figure 8 FAMIS 1 results: *a* (top left): $(\hat{a}_2, \hat{f}_2)$, *b* (top right): $(\hat{a}_3, \hat{f}_3)$, *c* (bottom left): $(\hat{a}_1, \hat{f}_1)$, *d* (bottom right): superimposition of the three factors

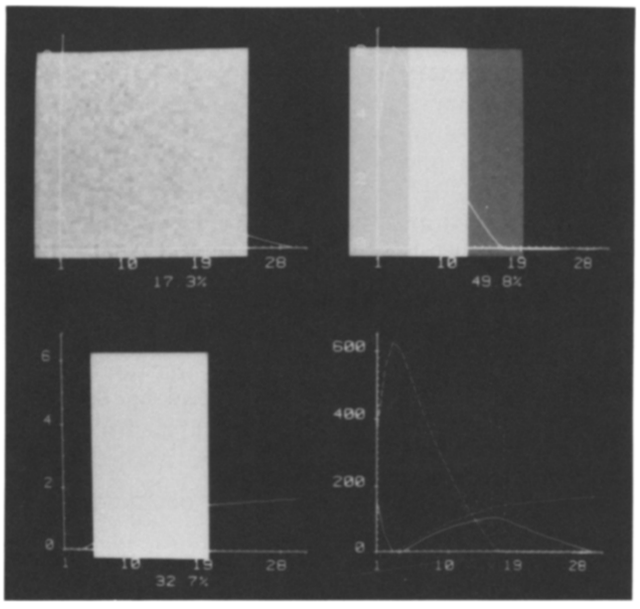

Figure 9 FAMIS 2 results: *a* (top left): $(\hat{a}_2, \hat{f}_2)$, *b* (top right): $(\hat{a}_1, \hat{f}_1)$, *c* (bottom left): $(\hat{a}_3, \hat{f}_3)$, *d* (bottom right): superimposition of the three factors

FAMIS 3 provides a satisfactory solution (*Figure 10*) by combining a relevant initialization (in $\mathbb{S}$ including trixels described by the only function f_2) with powerful constraints related to factors (fixed factor $\hat{f}_1$) and factor images (fixed factor images $\hat{a}_2$ and $\hat{a}_3$). Notice that the same powerful constraints used after an initialization in $\mathbb{S}^*$ do not lead to a correct solution, since f_2 is not initially properly estimated.

DISCUSSION

The conventional model underlying factor analysis of medical image sequences is revised and split up into a

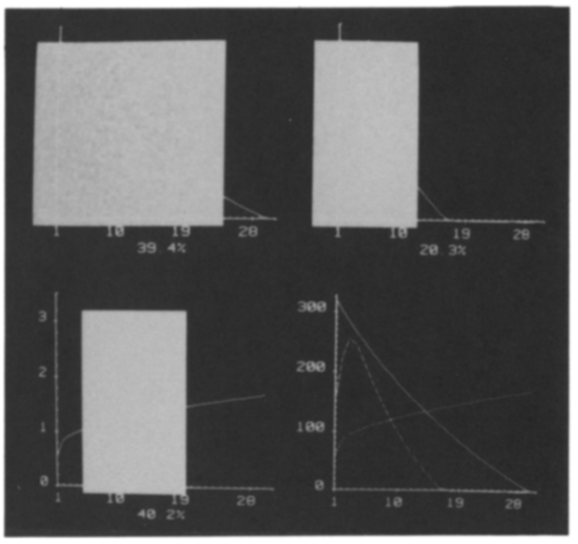

Figure 10 FAMIS 3 results: *a* (top left): $(\hat{a}_2, \hat{f}_2)$, *b* (top right): $(\hat{a}_1, \hat{f}_1)$, *c* (bottom left): $(\hat{a}_3, \hat{f}_3)$, *d* (bottom right): superimposition of the three factors

statistical model and a physical one. The introduction of a statistical model for medical image sequences, the fixed effect model, provides a theoretical basis for the choice of the metric to be used for the orthogonal analysis of FAMIS. When applying this model to scintigraphic data, it is shown that the optimal orthogonal decomposition is obtained by a correspondence analysis[20]. The interesting property of CA for our present purpose is that this decomposition treats the rows (i.e. trixels) and the columns (i.e. images) of the data matrix in the same way: a symmetrical role is given to trixels and images. To keep this symmetry, two hypotheses must be written to solve the physical model of FAMIS: the first one is related to the fundamental functions, while the second concerns the fundamental spatial distributions. Each of these hypotheses yields specific normalizations for factors and factor images. However, the hypotheses and induced normalizations can be mixed to derive a single solution for oblique analysis. This iterative method does not give any advantage to trixels or images. Up to now, all authors solved the physical model in the function space except for Samal *et al.*, who consider the image space[11,14,15]. No connection between these two approaches has been stated yet. The symmetrical model and solution unify these two formulations of FAMIS.

The only remaining asymmetry results from the initialization of the iterative procedure. It can begin by first estimating either the fundamental functions or the fundamental spatial distributions. The choice of the space in which the initialization is performed (function space or image space) strongly affects the final results of FAMIS. Indeed, the non-negativity constraints alone do not guarantee a unique solution for oblique analysis. The solution found in the study space then corresponds to the apices of the polytope which is closest to the starting polytope, and such that the non-negativity constraints are satisfied. As the apices of the starting polytope correspond to trixels (in the function space) or images (in the image space) of the processed image sequence, the better space to carry out the initialization step depends upon the processed data: when they include some trixels described by one single function, this function is properly estimated during the initialization step if it is performed in the function space. Conversely, if some images in the sequence contain only one fundamental spatial distribution, the most appropriate space for the initialization is the image space (see the first example discussed above). This result shows that a prior examination of the data before FAMIS is essential for a relevant choice of the initialization space.

It is well known that, in most studies, some *a priori* knowledge other than the non-negativity must be taken into account to improve FAMIS performances[12,22]. Numerous methods have been proposed to find the unique fundamental decomposition[21]. Some of them use knowledge about functions as constraints in the function space[8–10,17,23]. Others use knowledge about spatial distributions as constraints in the image space[11,14,15]. Lastly, other methods are based on knowledge related to the fundamental spatial distributions but expressed as constraints in the function space[24–26]. However, no method uses knowledge related to both fundamental functions and spatial distributions. The unified approach we propose deals with these two kinds of knowledge by means of the target apex seeking and the restoration of fixed poles and/or fixed image poles. As the introduction of these two types of constraints is sometimes necessary to achieve the accurate solution (see the second example discussed above), their simultaneous control should allow FAMIS to properly solve an increasing number of studies.

CONCLUSION

We have proposed a unified formulation and solution for FAMIS applied to scintigraphic data. It merges the solution in the function space and in the image space, and manages not only non-negativity constraints, but also *a priori* knowledge related to both fundamental functions and spatial distributions. The interest and the potentialities of this approach have been illustrated on simulated data. Its application to real studies is under investigation, particularly for problems in which *a priori* knowledge about functions and images is available. For instance, for scatter correction by FAMIS, some information related to the photopeak is known[21], and the image sequence can be acquired in a spectral domain such that some images correspond to one fundamental spatial distribution alone.

REFERENCES

1 Barber, D C 'The use of principal components in the quantitative analysis of gamma camera dynamic studies', *Phys. Med. Biol.*, Vol 25 No 2 (1980) pp 283–292

2 Bazin, J P, Di Paola, R, Gibaud, B, Rougier, P and Tubiana, M 'Factor analysis of dynamic scintigraphic data as a modelling method: An application to the detection of the metastases', in Di Paola, R and Kahn, E (eds.), *Information Processing in Medical Imaging*, INSERM, Paris, France (1980)

3 Di Paola, R, Bazin, J P, Aubry, F, Aurengo, A, Cavailloles, F, Herry, J Y and Kahn, E 'Handling of dynamic sequences in nuclear medicine', *IEEE Trans. Nucl. Sci.*, Vol 29 No 4 (1992) pp 1310–1321

4 Cavailloles, F, Morvan, D, Boudet, F, Bazin, J P and Di Paola, R 'Factor analysis of dynamic structures as an aid for vesicoureteral reflux diagnosis', *Contr. Nephrol.*, Vol 56 (1987) pp 238–242

5 Bonnerot, V, Charpentier, A, Frouin, F, Kalifa, C, Vanel, D and Di Paola, R 'Factor analysis of dynamic MR imaging in predicting the response of osteosarcoma to chemotherapy', *Invest. Radiol.*, Vol 27 No 10 (1992) pp 847–855

6 Frouin, F, Bazin, J P, Di Paola, M, Jolivet, O and Di Paola, R 'FAMIS: a software package for functional feature extraction from biomedical multidimensional images', *Comput. Med. Im. Graph.*, Vol 16 No 2 (1992) pp 81–91

7 Gagnon, D, Todd-Pokropek, A, Arsenault, A and Dupras, G 'Introduction to holospectral imaging in nuclear medicine for scatter subtraction', *IEEE Trans. Med. Imag.*, Vol 8 No 3 (1989) pp 245–250

8 Mas, J, Hannequin, P, Ben Younes, R, Bellaton, B and Bidet, R 'Scatter correction in planar imaging and SPECT by constrained factor analysis of dynamic structures (FADS)', *Phys. Med. Biol.*, Vol 35 No 11 (1990) pp 1451–1465

9 Buvat, I, Frouin, F, Ricard, M, Bazin, J P, Aubert, B and Di Paola, R 'Compton-scattered correction by constrained factor analysis of spectral structures', in Schmidt, H A E and van der Schoot, J B (eds.), *Nuclear Medicine*, Schattauer Verlag, Stuttgart (1991)

10 Nijran, K S and Barber, D C 'Factor analysis of dynamic function studies using *a priori* physiological information', *Phys. Med. Biol.*, Vol 31 No 10 (1986) pp 1107–1117

11 Samal, M, Karny, M, Surova, H, Marikova, E and Dienstbier, Z 'Rotation to simple structure in factor analysis of dynamic radionuclide studies', *Phys. Med. Biol.*, Vol 32 No 3 (1987) pp 371–382

12 Nijran, K S and Barber, D C 'The importance of constraints in factor analysis of dynamic studies', in de Graaf, C N and Viergever, M A (eds.), *Information Processing in Medical Imaging*, Plenum Press, New York (1988)

13 Nakamura, M, Suzuki, Y and Kobayashi, S 'A method for recovering physiological components from dynamic radionuclide images using the maximum entropy principle: a numerical investigation', *IEEE Trans. Biomed. Eng.*, Vol 36 No 9 (1989) pp 906–917

14 Samal, M, Surova, H, Karny, M, Marikova, E, Penicka, P and Dienstbier, Z 'The reality and meaning of physiological factors', in De Graaf, C and Viergever, M (eds.) *Information Processing in Medical Imaging*, Plenum Press, New York (1988)

15 Samal, M, Karny, M, Surova, H, Penicka, P, Marikova, E and Dienstbier, Z 'On the existence of an unambiguous solution in factor analysis of dynamic studies', *Phys. Med. Biol.*, Vol 34 No 2 (1989) pp 223–228

16 Caussinus, H 'Models and uses of principal component analysis', in de Leeuv, J (ed.), *Multidimensional Data Analysis*, DSWO Press, Leiden (1986)

17 Barber, D C and Nijran, K S 'Factor analysis of dynamic radionuclide studies', *Proc. 3rd World Congress of Nuclear Medicine and Biology* (Raynaud, C, ed.), WFNMB Vol 1, France (1982) pp 31–34

18 Kendall, M G and Stuart, A *The Advanced Theory of Statistics*, Charles Griffin, London (1967)

19 Greenacre, M J *Theory and Applications of Correspondence Analysis*, Academic Press, London (1989)

20 Benali, H, Buvat, I, Frouin, F, Bazin, J P and Di Paola, R 'Statistical model for the determination of the optimal metric in factor analysis of medical image sequences (FAMIS)', *Phys. Med. Biol.*, Vol 38 No 8 (1993) pp 1065–1080

21 Buvat, I, Benali, H, Frouin, F, Bazin, J P and Di Paola, R 'Target apex-seeking in factor analysis of medical image sequences', *Phys. Med. Biol.*, Vol 38 No 1 (1993) pp 123–138

22 Houston, A S and Nijran, K S 'Constraint problems in factor analysis of dynamic structures in nuclear medicine', *IEE 3rd Int. Conf. on Image Process*, IEE, UK (1989) pp 333–337

23 Nijran, K S and Barber, D C 'Towards automatic analysis of dynamic radionuclide studies using principal-components factor analysis', *Phys. Med. Biol.*, Vol 30 No 12 (1985) pp 1315–1325

24 Houston, A S 'The use of set theory and cluster analysis to investigate the constraint problem in factor analysis in dynamic structures (FADS)', in Bacharach, S L (ed.), *Information Processing in Medical Imaging*, Martinus Nijhoff, Dordrecht (1986)

25 Houston, A S 'The use of cluster analysis and constrained optimisation techniques in factor analysis of dynamic structures', in Viergever, M A and Todd-Pokropek, A E (eds.), *Mathematics and Computer Science in Medical Imaging*, Springer-Verlag, Berlin (1988)

26 Van Daele, M, Joosten, J, Devos, P, Vandecruys, A, Willems, J L and De Roo, M 'Background correction in factor analysis of dynamic scintigraphic studies: necessity and implementation', *Phys. Med. Biol.*, Vol 35 No 11 (1990) pp 1477–1485